Accuracy and Reproducibility of Assessing Patent Foramen Ovale on Coronary Computed Tomographic Angiography: A Comparison with Transesophageal Echocardiography

Li Xiong
Wuhan University Zhongnan Hospital, Department of ultrasound
Yingting Zeng
Wuhan University Zhongnan Hospital Department of Radiology: Wuhan University Zhongnan Hospital Medical Imaging Centre
Tian Gan
Wuhan university zhongnan hospital, Department of ultrasound
Feifei Yan
Wuhan university zhongnan hospital, Department of ultrasound
Jiao Bai
Wuhan university zhongnan hospital, Department of ultrasound
Yanbin Shi
Wuhan University Zhongnan Hospital Department of Radiology: Wuhan University Zhongnan Hospital Medical Imaging Centre
Xiaoyue Zhou
MR Collaboration, Siemens Healthcare Ltd.
Yu Wu
Guangzhou Women and Children's Medical Center, Department of Radiology
Xiaochun Zhang (zxcylxyr@163.com)
Guangzhou Women and Children's Medical Center

Research Article

Keywords: Coronary CT angiography, Patent foramen ovale, Transesophageal echocardiography, Contrast

Posted Date: June 22nd, 2021

DOI: https://doi.org/10.21203/rs.3.rs-602840/v1

Abstract

This study was undertaken to determine if coronary computed tomographic angiography (CCTA) can help to assess patent foramen ovale (PFO) with high accuracy and reproducibility when compared to Transesophageal Echocardiography (TEE). In total, 75 patients (31 men, 44 women; mean age, 45 ± 9 years) with suspected PFO were evaluated using coronary CCTA and TEE. PFO tunnel length (TL) and the opening diameter of the left atrial entrance (ODLAE) and right atrial entrance (ODRAE), as well as contrast shunt (if present due to PFO), were measured by both modalities. PFO was detected in 67 patients with TEE. The sensitivity for the detection of PFO with CCTA was 85.3%; specificity, 71.4%; positive predictive value, 96.7%; and negative predictive value, 33.3%. Both modalities demonstrated good agreement in measuring TL and ODLAE of PFO. However, the ODRAE of TEE was different from that of CCTA (1.14 ± 0.4 mm and 1.45 ± 0.5 mm, respectively, p = 0.04). The intraobserver and interobserver variability and agreement for TL, ODRAE, and ODLAE of PFO were excellent between the two measurements. CCTA provided a method for detection of PFO with high accuracy and reproducibility compared with TEE. Therefore, CCTA is a practical and efficient alternative to TEE for PFO diagnosis.

Introduction

The foramen ovale is located in the fossa ovalis of the atrial septum, and it is a channel that delivers venous blood from the right atria to the left atria in the fetus. This channel usually closes after birth. However, patent foramen ovale (PFO) is prevalent in nearly 25% of adults [1]. PFO has been correlated with the occurrence of various clinical syndromes, including cryptogenic stroke, migraines, and paradoxical embolism [2–3]. Therefore, the detection of PFO is clinically important.

Transthoracic echocardiography may be sufficient to detect a PFO as it shows the left to right shunt of blood through this channel [4]. However, transthoracic echocardiography is dependent on imaging quality. If the patient is overweight or has chronic obstructive pulmonary disease, the left to right shunt is not clearly visualized due to unsatisfactory imaging. Transcranial Doppler can also assess the severity of the right-to-left shunt [5]. However, transcranial Doppler is unable to differentiate a cardiac from a pulmonary right-to-left shunt and does not provide any information on cardiac anatomy. Transesophageal echocardiography (TEE) is the gold standard for the diagnosis of PFO [6]. Although TEE can evaluate the size and morphology of PFO, it is limited by the fact that it is a semi-invasive examination. Some patients, particularly children and the elderly, cannot tolerate the TEE probe being in the esophagus.

Coronary computed tomography angiography (CCTA) has high resolution images. In addition to its use in imaging coronary arteries, it can also be used to visualize other cardiac structures, such as the interatrial septum [7]. In CCTA, the routine method of contrast agent injection, coupled with a saline chaser to wash out the right side of the heart, allows the anatomy of the left side of the heart to be assessed, including the interatrial septum [8–9]. With this technique, demonstration of a left-to-right PFO shunt is possible, and no provocative test is required.

The purpose of our study was to demonstrate the anatomical structure of the PFO and to detect left-to-right shunts by using CCTA with reference to TEE.

Material And Methods

Study population

Between February 2019 and July 2020, we studied 75 clinically suspected PFO patients (31 men, 44 women: mean age, 45 ± 9 years) using consecutive CCTA and TEE examinations. Exclusion criteria included patients with severe coronary artery stenosis by CCTA and ASD by TEE. Clinical characteristics of the patients were collected from complete questionnaires and electronic medical records (Table 1). Of them, 56 patients had headache, 32 lacunar infarction and 25 recent stroke.

This study was approved by our medical school Institutional Review Board (IRB). Informed consent was exempted due to the retrospective study.

TEE examination

TEE examination was performed with a 6-VT real-time 3D transducer (Vivid E95, GE Medical Systems, Horten, Norway) using a standard technique. Patients underwent a comprehensive TEE study including two-dimensional imaging and color Doppler flow imaging of the PFO and agitated saline contrast test. The agitated saline contrast test was performed with 10 mL of agitated saline (a mixture of 9 mL of saline with 1mL of air) administered through an antecubital vein. The contrast test was positive by bubble visualization in the left atrium within three cardiac cycles following the Valsalva maneuver. PFO was confirmed on TEE by visualization of the gap between the septum primum and septum secundum and demonstration of interatrial shunting either by color Doppler imaging or saline contrast. Using two-dimensional imaging, we measured the tunnel length (TL) and opening diameter of the left atrial entrance (ODLAE) and right atrial entrance (ODRAE) of the PFO (Fig 1). All the TEE images were saved and analyzed later by two experienced echocardiography doctors who were blind to the clinical data.

CT scan protocol

All CT examinations were performed using 64-detector scanners (the SIEMENS dual-source CT, SOMATOM Definition system, Erlangen, Germany). Before the scan, the patients were required to fast for more than four hours. Strict breathing technique training (inhale, exhale, or breath-hold, according to the machine instructions) and heart rate control (<70/min) were used to avoid respiratory and motion artifacts that might affect image quality.

ECG monitoring was used, and venous access was established. The coronary artery calcification score was evaluated before the contrast injection. A bolus of 65-90 ml iodixanol (320 mg/ml), followed by 30-50 mL saline solution, was injected into an antecubital vein at a flow rate of 5-6 mL/s. The conventional method of contrast injection, coupled with a saline tracker to wash off the right side of the heart and assess the anatomy of the left side of the heart, allowed for PFO shunting from left-to-right to be

demonstrated. The region of interest (ROI) was set in the ascending aorta, and the scan would be triggered after a delay of 4 s when the CT value reached 100 Hu.

The scan range extended from tracheal bifurcation to the cardiac diaphragmatic side. Data were acquired using retrospective electrocardiography gating with the following parameters: 64 × 0.6 mm detector collimation, 0.33 s gantry rotation time, 0.20-0.46 pitch adapted to the heart rate, 120 kVp tube voltage, and automatic tube current.

CT data analysis and measurement

Multiplanar reformations of the images (short-axis, two-chamber, and four-chamber views) were rendered and evaluated on the Carestream Vue PACS workstation (Version 11.3.6.1156, Shanghai, China). All the image series were obtained at mid-diastole, and the best series that showed the flap valve of the septum primum, PFO shunt, and its direction were selected for the measurements. Image analysis and measurement were performed independently by two radiologist with cardiovascular CT diagnosis experience. PFO was considered to be present if a contrast jet from the contrast-filled left atrium to the saline-filled right atrium toward the inferior vena cava with a tunnel-like appearance of the interarterial septum was detected. Measurement indicators included the length of the flap valve tunnel, diameters of the tunnel at the left atrium side (diameter-A), and diameters of the tunnel at the entrance into the right atrium (diameter-B) (Fig 2). The images were magnified, and each distance was measured twice.

With the four-chamber view as a reference, sagittal-oblique images perpendicular to the interatrial septum were obtained, demonstrating the channel-like appearance of the interatrial septum. FFV length, PFO tunnel diameters (diameter-A and diameter-B), and shunt existence (Fig 3) were evaluated in the sagittal oblique images. The length of FFV and the diameter-A were measured from its free margin, and diameter-B was measured at the entrance into the right atrium.

Variability analysis

The interobserver variability and accuracy of TL, ODLAE, and ODRAE of the PFO by CCTA and TEE images were initially analyzed in 20 randomly selected patients by two qualified radiologists and echocardiography experts, who were blinded to the results of the initial study. To calculate the intraobserver variability in the CCTA and TEE, imaging assessment of the PFO parameters was repeated on the same data set after a delay of at least one month by the same investigator in 20 randomly selected patients.

Statistical analysis

Statistical analysis was performed using commercially available SPSS software (Version19.0, IBM, Armonk, NY, USA). All the data were presented as mean ± standard deviation. The correlation of function parameters between CCTA and TEE imaging was tested using a paired t-test and linear regression analysis with Pearson's correlation coefficient. Agreement of inter/intraobserver variability was determined by an inter-rater agreement (kappa), and weighted kappa (k) values were calculated (<0.40:

poor agreement, 0.40-0.75: fair to good, and >0.75: excellent). The accuracy of PFO shunt contrast present on CCTA was assessed by a diagnostic test, and the sensitivity (Sen) (%), specificity (Spe) (%), accuracy (Acc) (%), negative predictive value (NPV) (%), and positive predictive value (PPV) (%) were calculated. The significance of the biases was tested using a paired 2-sided t-test. Statistical significance was demonstrated when the p-value was less than 0.05.

Results

1. A comparison of PFO parameters between CCTA and TEE

The mean tunnel length (TL) and the opening diameter of the ODLAE and ODRAE of the PFO measured on CCTA and TEE imaging are summarized in Table 2. There were no statistically significant differences in the TL (12.16 ± 4.4 and 11.25 ± 4.0, respectively, p=0.78) or ODLAE (1.24 ± 0.5 and 1.36 ± 0.5, respectively, p=0.79) between the two modalities. However, the results for the ODRAE (1.14 ± 0.4 and 1.45 ± 0.5, respectively, p=0.04) were significantly different (Table 2).

2. Intraobserver and interobserver variability

The interobserver and intraobserver agreement in CCTA and TEE imaging for the TL, ODLAE, and ODRAE of the PFO were excellent. Therefore, there were no significant differences between the CCTA and TEE imaging for the interobserver and intraobserver agreements (p>0.05) (Table 3).

3. The accuracy of left to right shunt assessments for PFO on CCTA

PFO was diagnosed in 68 (90%) of the 75 patients using TEE. On the CT images, a contrast agent jet from the left atrium to the right atrium was detected in 60 patients. Fifty-eight of the 60 patients in which shunt was found on CTTA were diagnosed with a PFO on TEE. The sensitivity of this CT finding was 85.3%; specificity, 71.4%; PPV, 96.7%; and NPV, 33.3% (Table 4, Figs 3 and 4).

Discussion

This study demonstrates that CCTA has a high diagnostic performance for the detection of PFO compared to TEE. In addition, CCTA provides a method for the quantification of tunnel length and opening diameter of the left atrial entrance and right atrial entrance of the PFO with high reproducibility and excellent agreement with TEE.

Information about PFO parameters is clinically important for occluder therapy,some research has indicated the Amplatzer PFO Occluder has various sizes to suit variety of anatomies including PFOs that are associated with TL, ODLAE and ODRAE. [10]. PFO is known to be prevalent in nearly 25% of the adult population and has been correlated with a variety of clinical syndromes, including cryptogenic stroke, migraines, sleep apnea, and deep-sea diving-associated decompression illness [2, 3, 11–12]. Much research has shown that a chemical substance or tiny thrombus from the venous circulation can cross

the PFO tunnel between the right and left atria to generate a variety of clinical syndromes [13–14]. Another observational study suggested that a PFO tunnel with a shorter distance may be more prone to interatrial shunting [15]. Many clinical results have shown that percutaneous PFO closure is safe and effective as a treatment of choice for clinical syndrome prevention in such patients [10]. In addition, some researchers have demonstrated that the choice of the occluder size should be made suitable for PFO tunnel length (TL) and the thickness of the septum secundum that is associated with the ODLAE and ODRAE. The size of the occluder needs to be made available for a range of PFO anatomies, or it will potentially lead to complications [16]. Therefore, the TL, ODLAE, and ODRAE of the PFO are valuable for occluder therapy.

In this study, we found no statistically significant differences in the TL or ODLAE between the CCTA and TEE, but there was a difference with the ODRAE. TEE and CCTA rely on fundamentally different principles for measuring the ODRAE of the PFO. TEE is used to measure the diameter by two-dimension imaging, whereas CCTA is used to measure the diameter by detecting the contrast agent from left-to-right shunting in the resting state. Usually, leakage of contrast agent from the left cardiac chamber appears as a detectable contrast change in the right cardiac chamber, whereas contrast agent at the right atrial exit can be easily detected on CT images [17]. Hence, a contrast agent is clearly specific and present in the TL and ODLAE but is divergent and indistinct in the ODRAE.

The left-to-right CCTA shunt analysis demonstrated high sensitivity, specificity, accuracy, and positive predictive value. Our results were similar to those shown by Kim [15] et al.; however, the low negative predictive value has not been previously reported. There are two possible reasons for this difference. First, the shunts were only detected by CCTA between routine mid-diastolic phase images and/or end-systolic phase images; systolic phase images were difficult to evaluate due to dose modulation, whereas shunts could be detected in real-time using whole cycles with TEE. Second, TEE is used to diagnose PFO by detecting right-to-left shunt during Valsalva maneuver, whereas CT is used to diagnose PFO by detecting left-to-right shunting in the resting state when certain left-to-right shunting is limited or absent.

In conclusion, this study demonstrates that CCTA has a high diagnostic performance for the detection of PFO compared to TEE. Furthermore, CCTA provides a method for the quantification of tunnel length and opening diameter of the left atrial entrance and right atrial entrance of the PFO with high reproducibility and excellent agreement with TEE.

Declarations

Funding: Not applicable.

Conflicts of interest: The authors declare that they have no competing interests.

Ethics approval: Our study was approved by the ethical committee.

Consent to participate: Informed consent was exempted due to the retrospective study.

References

1. Hara H, Virmani R, Ladich E, Mackey-Bojack S, Titus J, Reisman M, Gray W, Nakamura M, Mooney M, Poulose A, Schwartz RS (2005) Patent foramen ovale: current pathology, pathophysiology, and clinical status. J Am Coll Cardiol 46(9): 1768-1776. https://doi.org/10.1016/j.jacc.2005.08.038
2. Knauth M, Ries S, Pohimann S, Kerby T, Forsting M, Daffertshofer M, Hennerici M, Sartor K (1997) Cohort study of multiple brain lesions in sport divers: role of a patent foramen ovale. BMJ 314(7082): 701-705. https://doi.org/10.1136/bmj.314.7082.701
3. Godart F, Rey C, Prat A, Vincentelli A, Chmaït A, Francart C, Porte H (2000) Atrial right-to-left shunting causing severe hypoxaemia despite normal right-sided pressures: report of 11 consecutive cases corrected by percutaneous closure. Eur Heart J 21(6): 483-489. https://doi.org/10.1053/euhj.1999.1944
4. Silvestry FE, Cohen MS, Armsby LB, Burkule NJ, Fleishman CE, Hijazi ZM, Lang RM, Rome JJ, Wang Y (2015) Guidelines for the echocardiographic assessment of atrial septal defect and patent foramen ovale: from the American Society of Echocardiography and Society for Cardiac Angiography and Interventions. J Am Soc Echocardiogr 28(8): 910-958. https://doi.org/10.1016/j.echo.2015.05.015
5. Mojadidi MK, Roberts SC, Winoker JS, Romero J, Goodman-Meza D, Gevorgyan R, Tobis JM(2014) Accuracy of transcranial Doppler for the diagnosis of intracardiac right-to-left shunt: a bivariate meta-analysis of prospective studies. JACC Cardiovasc Imag 7(3): 236-250. https://doi.org/10.1016/j.jcmg.2013.12.011
6. Hahn RT, Abraham T, Adams MS, Bruce CJ, Glas KE, Lang RM, Reeves ST, Shanewise JS, Siu SC, Stewart W, Picard MH (2013) Guidelines for performing a comprehensive transesophageal echocardiographic examination: recommendations from the American Society of Echocardiography and the Society of Cardiovascular Anesthesiologists. J Am Soc Echocardiogr 26(9): 921-964. https://doi.org/10.1016/j.echo.2013.07.009
7. Boxt LM, Lipton MJ, Kwong RY, Rybicki F, Clouse ME (2003) Computed tomography for assessment of cardiac chambers, valves, myocardium and pericardium. Cardiol Clin 21(4): 561-585. https://doi.org/10.1016/S0733-8651(03)00093-6
8. Saremi F, Attai SF, Narula J (2007) 64 Multidetector CT in patent foramen ovale. Heart 93(4). https://doi.org/10.1136/hrt.2006.097782
9. Cademartiri F, Mollet N, Lugt A, Nieman K, Pattynama PM, Feyter PJ, Krestin GP (2004) Non-invasive 16-row multislice CT coronary angiography: usefulness of saline chaser. Eur Radiol 14(2): 178-183. https://doi.org/10.1007/s00330-003-2188-x
10. Madhkour R, Wahl A, Praz F, Meier B (2019) Amplatzer patent foramen ovale occluder: safety and efficacy. Expert Rev Med Devic 16(3): 173-182. https://doi.org/10.1080/17434440.2019.1581060
11. Schuchlenz HW, Weihs W, Horner S, Quehenberger F (2000) The association between the diameter of a patent foramen ovale and the risk of embolic cerebrovascular events. Am J Med 109(6): 456-

462. https://doi.org/10.1016/S0002-9343(00)00530-1

12. Godart F, Rey C, Prat A, Vincentelli A, Chmaït A, Francart C, Porte H (2000) Atrial right-to-left shunting causing severe hypoxaemia despite normal right-sided pressures: report of 11 consecutive cases corrected by percutaneous closure. Eur Heart J 21(6): 483-489. https://doi.org/10.1053/euhj.1999.1944
13. Snijder RJ, Luermans JG, Heij AH, Thijs V, Schonewille WJ, Bruaene AV, Swaans MJ, Budts WI, Post MC (2016) Patent foramen ovale with atrial septal aneurysm is strongly associated with migraine with aura: a large observational study. J Am Heart Assoc 5(12): e003771. https://doi.org/10.1161/JAHA.116.003771
14. West BH, Noureddin N, Mamzhi Y, Low CG, Clouzzi AC, Shih EJ, Fleming RG, Saver JL, Liebeskind DS, Charles A, Tobis JM (2018) Frequency of patent foramen ovale and migraine in patients with cryptogenic stroke. Stroke 49(5): 1123-1128. https://doi.org/10.1161/STROKEAHA.117.020160
15. Kim YJ, Hur J, Shim CY, Lee HJ, Ha JW, Choe KO, Heo JH, Choi EY, Choi BW (2009) Patent Foramen Ovale: Diagnosis with Multidetector CT-Comparison with Transesophageal Echocardiography. Radiology 250(1): 61-67. https://doi.org/10.1148/radiol.2501080559
16. Giordano M, Gaio G, Santoro G, Palladino MT, Sarubbi B, Golino P, Russo MG (2019) Patent foramen ovale with complex anatomy: Comparison of two different devices (Amplatzer Septal Occluder device and Amplatzer PFO Occluder device 30/35). Int J Cardiol 279:47-50. https://doi.org/10.1016/j.ijcard.2018.10.053
17. Saremi F, Channual S, Raney A, Gurudevan SV, Narula J, Fowler S, Abolhoda A, Milliken JC (2008) Imaging of Patent Foramen Ovale with 64-Section Multidetector CT. Radiology 249(2): 483-492. https://doi.org/10.1148/radiol.2492080175

Tables

Table 1. Basic clinical characteristics of the study population (n = 75)

Characteristics	Value
Age (years)	53 ± 5
Males, n (%)	30 (38)
BMI, (kg/m^2)	23 ± 2.3
Hypertension, n (%)	12 (15)
Diabetes mellitus, n (%)	14 (18)
Dyslipidemia, n (%)	27 (35)
Smoker, n (%)	26 (33)
Coronary artery disease, n (%)	9 (15)
EF (%)	58 ± 9
DVT, n (%)	17 (22)
History of pulmonary disease, n (%)	13 (17)
Platypnea-orthodeoxia syndrome, n (%)	15 (19)
Migraine headache, n (%)	56 (72)
Lacunar infarction, n (%)	32 (41)
Recent stroke, n (%)	25 (32)

Data are presented as mean ± standard deviation or count (%).

BMI, body mass index; EF, ejection fraction; DVT, deep vein thrombosis.

Table 2. Patent foramen ovale parameters obtained with coronary computed tomographic angiography (CCTA) and transesophageal echocardiography (TEE)

	CCTA	TEE	P
TL (mm)	12.16 ± 4.4	11.25 ± 4.0	0.78
ODLAE (mm)	1.24 ± 0.5	1.36 ± 0.5	0.79
ODRAE (mm)	1.14 ± 0.4	1.45 ± 0.5	0.04

Data are presented as mean ± standard deviation.

TL, tunnel length; ODLAE, opening diameter of the left atrial entrance; ODRAE, opening diameter of the right atrial entrance.

Table 3. Intraobserver and interobserver variability of patent foramen ovale parameters obtained by coronary computed tomographic angiography (CCTA) and transesophageal echocardiography (TEE)

		Agreement of interobserve	Agreement of intra-observer
Tunnel L	CCTA	0.78	0.87
	TEE	0.79	0.83
LA D	CCTA	0.8	0.81
	TEE	0.82	0.79
RA D	CCTA	0.83	0.78
	TEE	0.85	0.77

Data are presented as mean ± standard deviation.

TL, tunnel length; ODLAE, opening diameter of the left atrial entrance; ODRAE, opening diameter of the right atrial entrance.

Table 4. Diagnosis of patent foramen ovale using coronary computed tomographic angiography (CCTA) and transesophageal echocardiography (TEE)

	PFO on TEE		
Shunt on CCTA	Present	Absent	Total
Present	58	2	60
Absent	10	5	15
Total	68	7	75

Figures

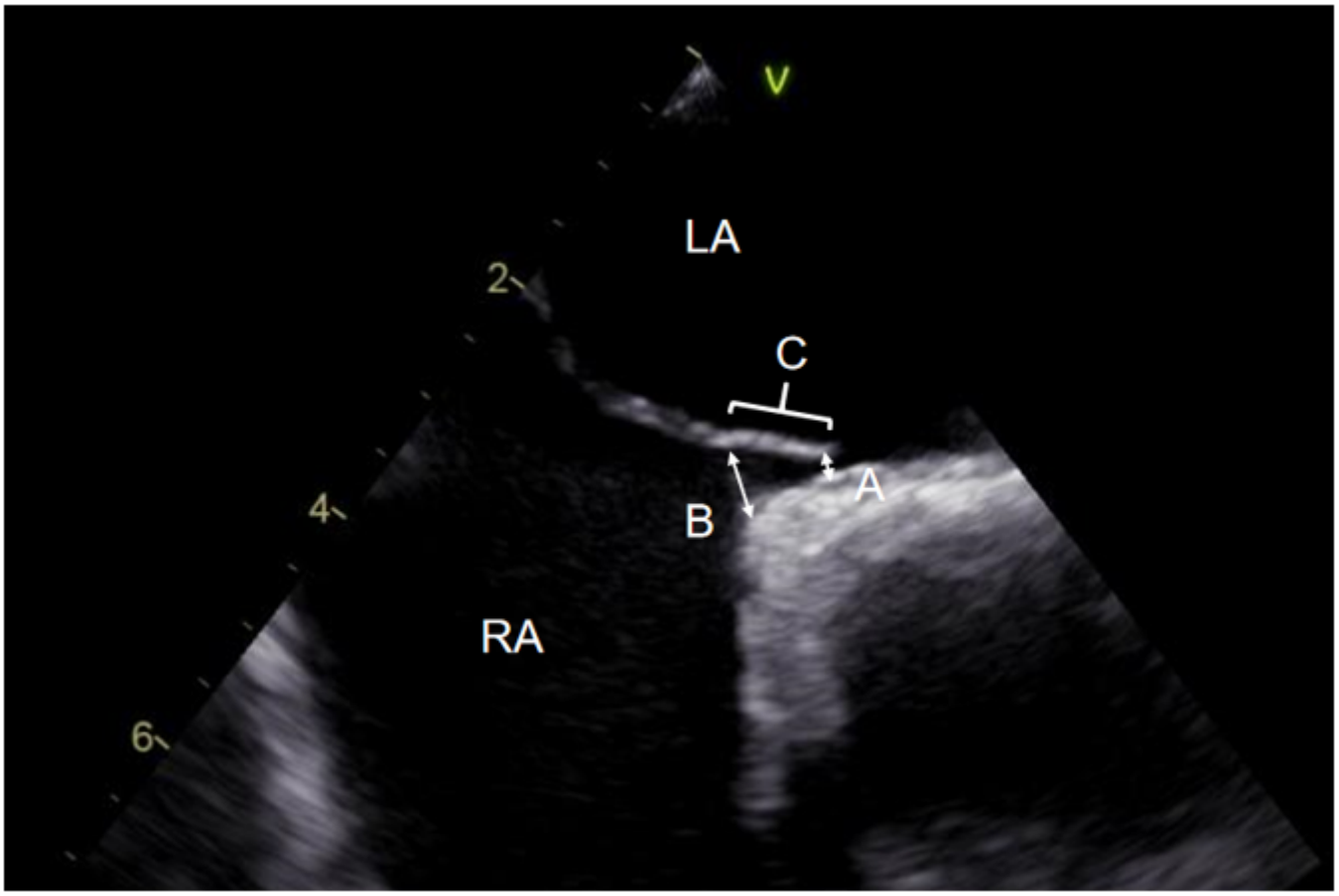

Figure 1

Patent foramen ovale (PFO) shown on 2-dimensional transesophageal echocardiography (TEE) imaging A: Opening diameter of left atrial entrance (ODLAE) B: Opening diameter of right atrial entrance (ODRAE) C: Tunnel length (TL) LA: Left Atrium; RA: Right Atrium

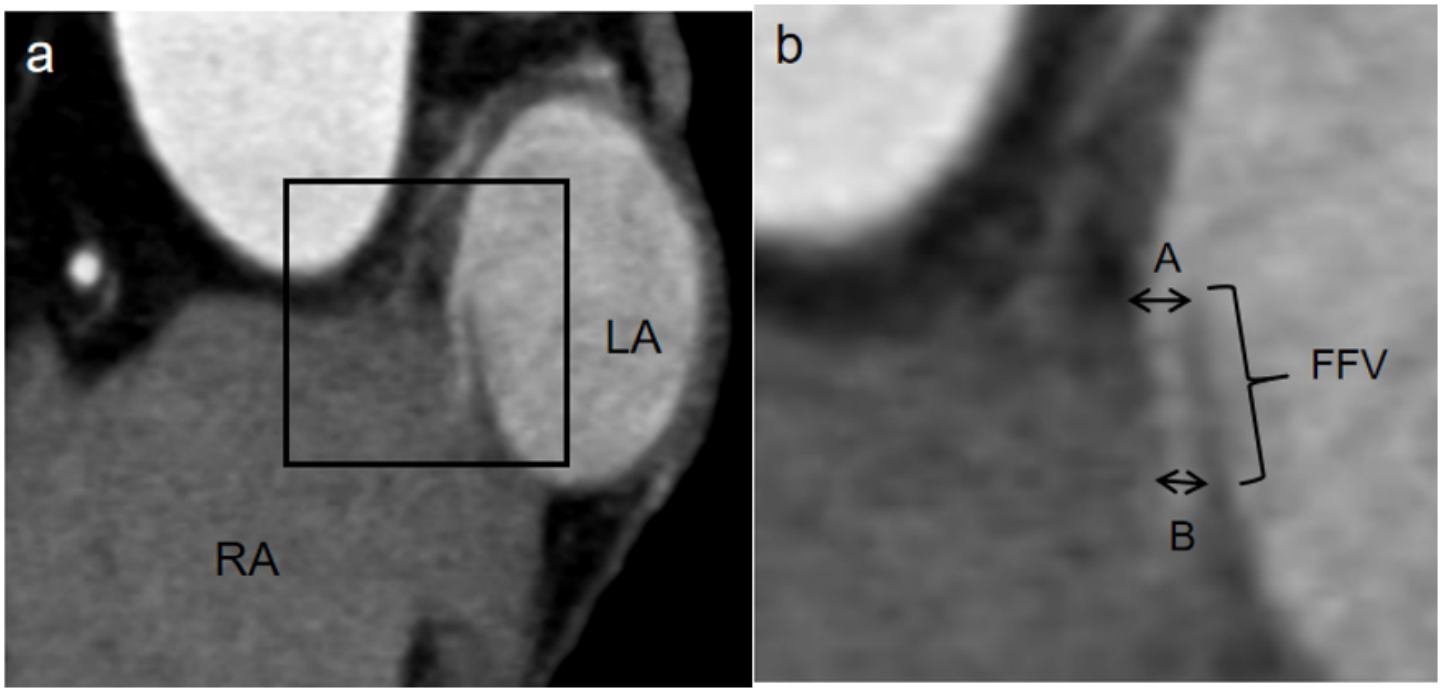

Figure 2

(a) Sagittal-oblique reformatted computed tomographic (CT) image of a 46-year-old man showing a well-developed patent foramen ovale (PFO). (b) Close-up view showing anatomic details. Length of free flap valve (FFV): from its free margin to the level of the superior rim of the fossa ovalis. Diameter-A: from its free margin to the interatrial groove. Diameter-B: diameter of the tunnel at the entrance into the right atrium.

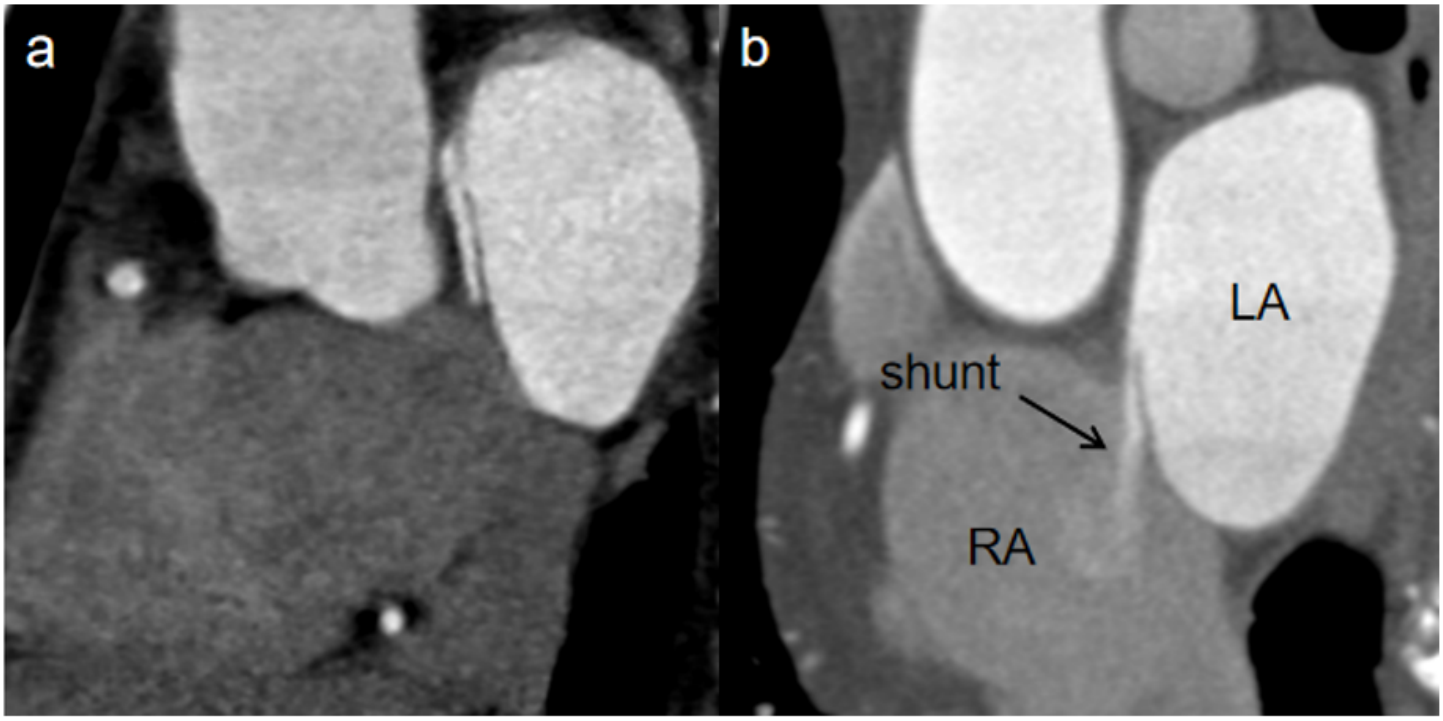

Figure 3

(a) A computed tomographic (CT) image of a 45-year-old man showing the channel-like appearance of the interatrial septum. (b) A CT image of a 61-year-old woman showing the shunt from the left atrium to the right atrium through the foramen ovale.

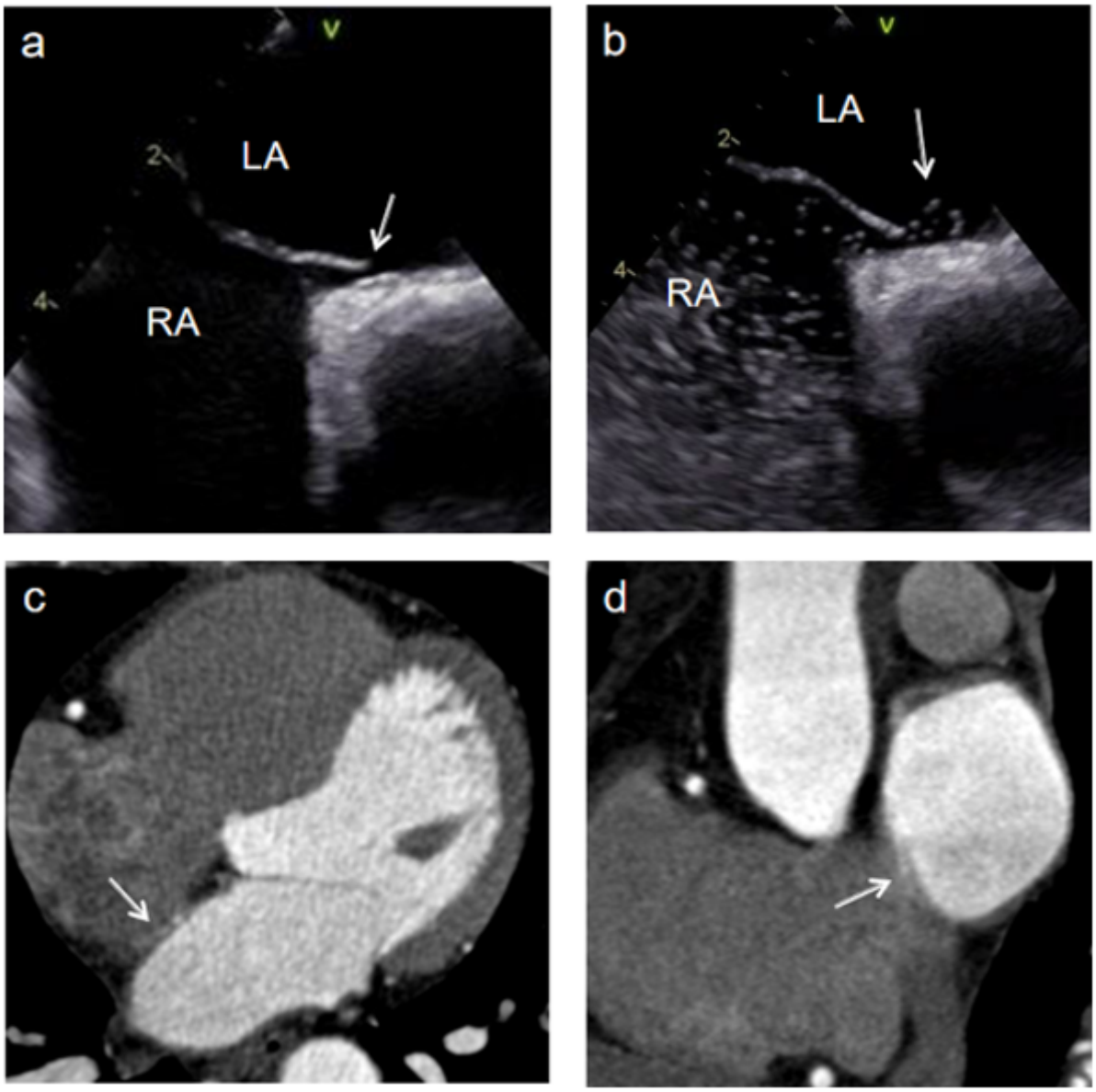

Figure 4

Patent foramen ovale (PFO) diagnosed using transesophageal echocardiography (TEE) in a 56-year-old woman. (a) 2-dimensional TEE image showing PFO open status (arrow). (b) TEE image with agitated saline injection and Valsalva maneuver reveals shunt from the right atrium (RA) to left atrium (LA) with appearance of microbubbles (arrow) in LA. (c) Axial and (d) oblique sagittal reformation CT images demonstrate the channel-like appearance of interarterial septum (IAS; arrow in c) and contrast agent jets from LA to RA (arrow in d).